Defense Threat Reduction Agency
8725 John J. Kingman Road, MS 6201
Fort Belvoir, VA 22060-6201

DTRA-TR-03-19

TECHNICAL REPORT

Development of a Regional 3-D Velocity Model of the Pakistan Region for Improved Seismic Event Location

Approved for public release; distribution is unlimited.

April 2006

DSWA01-98-C-0143

Delaine Reiter, et al.

Prepared by:
Weston Geophysical Corporation
57 Bedford Street
Suite 102
Lexington, MA 02420

Massachusetts Institute of Technology
Earth Resources Laboratory
42 Carleton Street
Cambridge, MA 02142

DESTRUCTION NOTICE

FOR CLASSIFIED documents, follow the procedures in DoD 5550.22-M, National Industrial Security Program Operating Manual, Chapter 5, Section 7 (NISPOM) or DoD 5200.1-R, Information Security Program Regulation, Chapter 1X.

FOR UNCLASSIFIED limited documents, destroyed by any method that will prevent disclosure of contents or reconstruction of the document.

Retention of this document by DoD contractors is authorized in accordance with DoD 5220.22M, Industrial Security manual.

PLEASE NOTIFY THE DEFENSE THREAT REDUCTION AGENCY, ATTN: IMMI, 8725 JOHN J. KINGMAN ROAD, MS-6201, FT. BELVOIR, VA 22060-6201. IF YOUR ADDRESS IS INCORRECT, IF YOU WISH IT DELETED FROM THE DISTRIBUTION LIST, OR IF THE ADDRESSEE IS NO LONGER EMPLOYED BY YOUR ORGANIZATION.

DISTRIBUTION LIST UPDATE

This mailer is provided to enable DTRA to maintain current distribution lists for reports. (We would appreciate you providing the requested information.)

- ❑ Add the individual listed to your distribution list.
- ❑ Delete the cited organization/individual.
- ❑ Change of address.

Note:
Please return the mailing label from the document so that any additions, changes, corrections or deletions can be made easily. For distribution cancellation or more information call DTRA/BDLMI (703) 767-4725.

NAME: _____

ORGANIZATION: _____

OLD ADDRESS	NEW ADDRESS
_____	_____
_____	_____
_____	_____

TELEPHONE NUMBER: ( ) _____

DTRA PUBLICATION NUMBER/TITLE	CHANGES/DELETIONS/ADDITONS, etc. *(Attach Sheet if more Space is Required)*
_____	_____
_____	_____
_____	_____

DTRA or other GOVERNMENT CONTRACT NUMBER: _____

CERTIFICATION of NEED-TO-KNOW BY GOVERNMENT SPONSOR (if other than DTRA):

SPONSORING ORGANIZATION: _____

CONTRACTING OFFICER or REPRESENTATIVE: _____

SIGNATURE: _____

DEFENSE THREAT REDUCTION AGENCY
ATTN: BDLMI
8725 John J Kingman Road, MS 6201
Fort Belvoir, VA 22060-6201

DEFENSE THREAT REDUCTION AGENCY
ATTN: BDLMI
8725 John J Kingman Road, MS 6201
Fort Belvoir, VA 22060-6201

REPORT DOCUMENTATION PAGE

Form Approved
OMB No. 0704-0188

1. REPORT DATE *(DD-MM-YYY)*	2. REPORT TYPE	3. DATES COVERED *(From - To)*
03 September 2003	Technical Report	

4. TITLE AND SUBTITL
Development of a Regional 3-D Velocity Model of the Pakistan Region for Improved Seismic Event Location (U)

5a. CONTRACT NUMBER
DSWA 01-98-C-0143

5b. GRANT NUMBER

5c. PROGRAM ELEMENT NUMBER
1310

6. AUTHOR(S)
Delaine Reiter, Michelle Johnson, Anca Rosca, Carolynn Vincent (WGC),
And William Rodi (MIT)

5d. PROJECT NUMBER
OS

5e. TASK NUMBER
OO

5f. WORK UNIT NUMBER
DH56417

7. PERFORMING ORGANIZATION NAME(S) AND ADDRESS(ES)

Weston Geophysical Corporation
57 Bedford Street, Suite 102
Lexington, MA 02420

Massachusetts Institute of Technology
Earth Resources Laboratory
42 Carleton St.
Cambridge, MA 02142

8. PERFORMING ORGANIZATION REPORT NUMBER

9. SPONSORING / MONITORING AGENCY NAME(S) AND ADDRESS(ES)
Defense Threat Reduction Agency
8725 John J. Kingman Rd., MS 6201
Fort Belvoir, VA 22060-6201

10. SPONSOR/MONITOR'S ACRONYM(S)
DTRA

11. SPONSOR/MONITOR'S REPORT NOS.
TR-03-19

12. DISTRIBUTION / AVAILABILITY STATEMENT
Approved for public release; distribution is unlimited.

13. SUPPLEMENTARY NOTES
This work was sponsored by the Defense Threat Reduction Agency under the RDT&E RMC Code B 1310 D 3E30 OS OO 56417 25904D.

14. ABSTRACT

In this report, we detail the development of a new regional 3-D tomographic P-wave velocity model (WINPAK3D) of a region in Southern Asia centered on Pakistan. Our primary goal in developing a 3-D model of the crust and upper mantle in this region is to improve regional seismic event location. A detailed initial Pn model was iteratively refined using a nonlinear, conjugate-gradients technique that adjusts the velocity model of model to minimize the misfit between calculated and observed travel times from multiple stations and events, subject to smoothness constraints. We compute the travel times and their sensitivities to the velocity structure with an extension of the 3-D Podvin-Lecomte (1991) method. Because the event locations are not fixed, we also relocate all events using a 3-D grid search location method after each update of the 3-D velocity model. The data set consisted of a suite of 535 events containing over 6,600 arrivals from the Engdahl, et al. (1998) database. Our results show that the new model better fits the data compared to both the initial model and the global 1-D IASP91 model. The root mean square (RMS) error for the updated 3-D model is 1.81, compared to 2.01 for the initial 3-D model and 2.42 for the IASP91 model.

15. SUBJECT TERMS
Regional seismic event location
Joint nonlinear tomography
Pakistan
3-D Velocity models

16. SECURITY CLASSIFICATION OF:			17. LIMITATION OF ABSTRACT	18. NUMBER OF PAGES	19a. NAME OF RESPONSIBLE PERSON
a. REPORT	b. ABSTRACT	c. THIS PAGE			19b. TELEPHONE NUMBER *(include area code)*
Unclassified	Unclassified	Unclassified	SAR	29	

CONVERSION TABLE

Conversion Factors for U.S. Customary to metric (SI) units of measurement.

MULTIPLY →	BY →	TO GET
TO GET ←	BY ←	DIVIDE

angstrom	1.000 000 x E -10	meters (m)
atmosphere (normal)	1.013 25 x E +2	kilo pascal (kPa)
bar	1.000 000 x E +2	kilo pascal (kPa)
barn	1.000 000 x E -28	meter^2 (m^2)
British thermal unit (thermochemical)	1.054 350 x E +3	joule (J)
calorie (thermochemical)	4.184 000	joule (J)
cal (thermochemical/cm^2)	4.184 000 x E -2	mega joule/m^2 (MJ/m^2)
curie	3.700 000 x E +1	*giga bacquerel (GBq)
degree (angle)	1.745 329 x E -2	radian (rad)
degree Fahrenheit	$t_k = (t°f + 459.67)/1.8$	degree kelvin (K)
electron volt	1.602 19 x E -19	joule (J)
erg	1.000 000 x E -7	joule (J)
erg/second	1.000 000 x E -7	watt (W)
foot	3.048 000 x E -1	meter (m)
foot-pound-force	1.355 818	joule (J)
gallon (U.S. liquid)	3.785 412 x E -3	meter^3 (m^3)
inch	2.540 000 x E -2	meter (m)
jerk	1.000 000 x E +9	joule (J)
joule/kilogram (J/kg) radiation dose absorbed	1.000 000	Gray (Gy)
kilotons	4.183	terajoules
kip (1000 lbf)	4.448 222 x E +3	newton (N)
kip/inch^2 (ksi)	6.894 757 x E +3	kilo pascal (kPa)
ktap	1.000 000 x E +2	newton-second/m^2 ($N-s/m^2$)
micron	1.000 000 x E -6	meter (m)
mil	2.540 000 x E -5	meter (m)
mile (international)	1.609 344 x E +3	meter (m)
ounce	2.834 952 x E -2	kilogram (kg)
pound-force (lbs avoirdupois)	4.448 222	newton (N)
pound-force inch	1.129 848 x E -1	newton-meter (N-m)
pound-force/inch	1.751 268 x E +2	newton/meter (N/m)
pound-force/foot^2	4.788 026 x E -2	kilo pascal (kPa)
pound-force/inch^2 (psi)	6.894 757	kilo pascal (kPa)
pound-mass (lbm avoirdupois)	4.535 924 x E -1	kilogram (kg)
pound-mass-foot^2 (moment of inertia)	4.214 011 x E -2	kilogram-meter^2 ($kg-m^2$)
pound-mass/foot^3	1.601 846 x E +1	kilogram-meter^3 (kg/m^3)
rad (radiation dose absorbed)	1.000 000 x E -2	**Gray (Gy)
roentgen	2.579 760 x E -4	coulomb/kilogram (C/kg)
shake	1.000 000 x E -8	second (s)
slug	1.459 390 x E +1	kilogram (kg)
torr (mm Hg, 0^0 C)	1.333 22 x E -1	kilo pascal (kPa)

*The bacquerel (Bq) is the SI unit of radioactivity; 1 Bq = 1 event/s.
**The Gray (GY) is the SI unit of absorbed radiation.

TABLE OF CONTENTS

LIST OF FIGURES AND TABLES

SUMMARY

In this report we detail the development of a new regional 3-D tomographic P-wave velocity model (WINPAK3D) of a region in Southern Asia centered on Pakistan. Our primary goal in developing a 3-D model of the crust and upper mantle in this region is to improve regional seismic event location. The initial model for the region was developed by integrating the results of more than 60 previous studies related to crustal and upper mantle velocity structure. We refined the model by applying a joint velocity tomography and event location procedure to a dataset of earthquakes in the region. The model was iteratively updated using a nonlinear, conjugate-gradients technique that adjusts the velocity model to minimize the misfit between calculated and observed travel times from multiple stations and events, subject to smoothness constraints. We compute the travel times and their sensitivities to the velocity structure with an extension of the 3-D Podvin-Lecomte (1991) method. Because the event locations are not fixed, we also relocate all events using a 3-D grid search location method after each update of the 3-D velocity model. The data set consisted of a suite of 535 events containing over 6,600 arrivals from the Engdahl *et al.* (1998) database. We performed several iterations of the nonlinear algorithm to invert for the *Pn* velocity as a function of latitude and longitude and then imposed a fixed rule for extrapolating this velocity into the upper mantle. Future extensions of the method will allow for more flexible changes in the upper crust and mantle portions of the model. Our results show that the new model better fits the data compared to both the initial model and the global 1-D IASP91 model. The root mean square (RMS) error for the the updated 3-D model is 1.81, compared to 2.01 for the initial 3-D model and 2.42 for the IASP91 model.

INTRODUCTION

An accurate estimate of the location of a seismic event is particularly important for monitoring potential nuclear explosions. Determining hypocenters for small seismic events ($m_b < 4.0$) with high accuracy is difficult because of limited recordings and complicated crustal structure at regional distances that is not accounted for in the standard global 1-D models such as the IASP91 model (Kennett and Engdahl, 1991). Precise regional location of seismic events requires a velocity model that accurately represents the real Earth structure, as systematic biases caused by unmodeled Earth structure are known to play an important role in earthquake location errors (e.g., Douglas, 1967; Dewey, 1972; Engdahl and Lee, 1976; Jordan and Sverdrup, 1981; Pavlis, 1992). Regional 3-D models that better represent the true Earth structure can be used to compute accurate travel times of regional seismic phases such as *Pn*, *Pg*, *Sn*, and *Lg*. Travel times calculated using 3-D models can then be used to develop source specific station corrections (SSSC's) that can be implemented by monitoring organizations to provide improved regional event locations. Our goal in this research project was to develop a regional model of the crust and upper mantle for the India-Pakistan region that will improve event location accuracy. We built our model for the India-Pakistan region by updating a detailed preliminary model through a joint, nonlinear velocity tomography and hypocenter relocation technique. In the following sections we describe first the inversion

algorithm followed by the application of the algorithm to a set of earthquake data surrounding a region centered on Pakistan contained inside 25-40° N and 60-75° E.

JOINT VELOCITY TOMOGRAPHY/EVENT LOCATION ALGORITHM DEVELOPMENT

The development of high-resolution, 3-D velocity models using regional earthquake data is complicated by the dependence of the model on mislocations of the earthquake hypocenters. Travel time measurements from earthquakes depend both on the earthquake locations and the earth's velocity structure. Hypocenter estimates are biased by errors in the velocity model. Conversely, tomographic images of the velocity structure derived from earthquake arrival times are affected by errors in the earthquake hypocenters. It has long been recognized that earthquake location and velocity imaging are coupled inverse problems. The problems separate only when sufficient prior data exists to constrain one set of parameters or the other, or in special geometries. Our study in Pakistan was motivated by the lack of prior information needed to decouple the location and velocity imaging problems. Furthermore, we wanted to use the wealth of information contained in local and regional earthquake data, whose source-receiver geometry prevents the separation of the problems. Our inversion algorithm jointly solves the nonlinear problem through the application of a conjugate gradient technique, which iterates over linear inversion steps that include updates of the hypocenters, velocities and ray paths. The technique explicitly addresses the coupling between the hypocenters and the velocity structure by computationally breaking down the large matrix that must be inverted for velocities and locations. This computational technique results in two separate smaller matrices which may be inverted separately, but still solve the simultaneous problem (Spencer and Gubbins, 1980; Rodi *et al.*, 1981).

Figure 1 is a simple flowchart of the algorithm we used to develop our new 3-D velocity model of the India-Pakistan region. There are three major components involved in our joint tomography/location procedure: 1) 3-D ray tracing to predict first arrival times using an enhanced version of the Podvin-Lecomte (P-L) method (1991); 2) a 3-D grid search location algorithm (GSEL) from Rodi and Toksöz (2000) to relocate events inside the appropriate velocity model; and 3) a linear conjugate gradient inversion algorithm to produce the updated velocity model inside each iteration of the overall nonlinear algorithm. In the next few subsections we describe the velocity model parameterization and each of the three major algorithmic components.

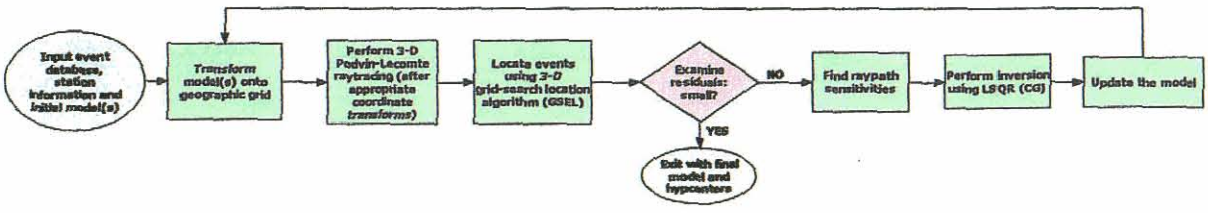

Figure 1: Simplified flowchart of the nonlinear joint tomography and location procedure used to develop the 3-D model of the region in and around Pakistan.

Velocity Model Parameterization

We parameterize our 3-D model of the Pakistan region in terms of a velocity vs. depth profile at each point on a geographic grid, which is sampled uniformly in latitude and longitude. At each geographic grid-point, the velocity profile is given as velocity/depth pairs at nodes ranging from sea level to a depth of 760 km. Discontinuities in velocity are allowed at the ocean bottom, Moho and the major mantle discontinuities (410 and 660 km depth in the IASP91 model). Using this parameterization also reduces the number of model parameters to be solved for in the inversion. One complication in using this geographically-defined velocity model is that our current implementation of the Podvin-Lecomte algorithm solves the eikonal equation in Cartesian coordinates for a flat-earth model. However, we have developed the algorithms for accurately mapping our geographic velocity model to a Cartesian block model required by the P-L algorithm and for mapping the 3-D Cartesian travel time grids and related ray path sensitivities back to geographic grids for use in the inversion.

Inversion Method

We formulate our inversion approach as follows: the unknowns are a vector $\mathbf{m}$ containing the velocity model parameters to be estimated and the hypocenters ($\mathbf{x}_j$) and origin times (t_j) of M events: ($\mathbf{x}_j$, t_j), $j = 1,..., M$. The data are arrival times, d_{ij}, from each event to a subset of N stations indexed as $i = 1,..., N$. The data and unknowns are related by

$$d_{ij} = t_j + T_i(\mathbf{x}_j;\mathbf{m}) + e_{ij}, \qquad (1)$$

where e_{ij} is the error in d_{ij} and T_i is a function that predicts the travel time to station i from an event hypocenter $\mathbf{x}_j$. This function depends on the model parameter vector $\mathbf{m}$. Our joint inversion criterion is to minimize an objective function of the form

$$\Psi(\mathbf{m}, \mathbf{x}_1, t_1, ..., \mathbf{x}_M, t_M) = \sum_{ij} | d_{ij} - t_j + T_i(\mathbf{x}_j;\mathbf{m}) |^2 / \sigma_{ij}^2 + \tau | \mathbf{Lm} |^2 \quad (2)$$

with respect to all the unknowns. Here, σ_{ij} is the standard deviation of e_{ij}. The second term of ψ imposes a smoothness constraint on the velocity model, where $\mathbf{L}$ is a

regularization operator and τ a regularization parameter. The operator **L** is a differencing operator that minimizes the spatial derivatives of the model velocity. The parameter τ determines the degree of model smoothness.

We perform the minimization of Ψ numerically using a combination of nonlinear conjugate gradient (NLCG) and grid-search techniques. The NLCG technique is used to update the model **m** iteratively along a sequence of computed search directions. Inside each NLCG iteration, three processes occur: 3-D ray tracing to predict travel times, a grid search location method to minimize ψ with respect to all the event hypocenters ($\mathbf{x}_j$) and origin times (t_j) with the model fixed, and a linear conjugate gradients method to update the velocity model **m**. The grid search for a given event is performed within a specified epicentral radius and depth range from its initial location, allowing us to handle events of varying ground-truth levels (e.g., GT0, GT5, GT15). The linear conjugate gradient method iteratively computes an optimal update to the current 3-D velocity model using the appropriate travel time tables and hypocenters for that model. This optimized update is then used as a search direction in the NLCG inversion.

We note that our joint inversion algorithm is fully nonlinear with respect to both the velocity model and event locations since travel time modeling and event relocation are performed for each update of **m**. We also note that we are currently solving only for the *Pn* velocity as a function of latitude and longitude and imposing a fixed rule for extrapolating this velocity into the upper mantle. Future extensions of our approach will implement more general model parameterizations to allow for changes in Moho depth and more general variations in upper mantle velocity.

Travel Time Calculation Using Podvin-Lecomte Ray Tracing

To determine the values of the travel time functions T_i, we evaluate $T_i(\mathbf{x}; \mathbf{m})$ for a fixed hypocenter by interpolating a travel time table stored on a 3-D hypocenter grid. This grid is created by applying the Podvin-Lecomte (P-L) finite-difference travel time algorithm (Lomax, 1999; Podvin and Lecomte, 1991) to the earth model defined by **m**, using the location of the *i*th station as the "source" in the calculation. The Podvin-Lecomte method solves the eikonal equation in a 3-D medium using a finite-difference approximation. It can accurately model different propagation modes, such as transmitted and diffracted body waves or head waves. It estimates accurate travel times in the presence of severe, arbitrarily-shaped velocity contrasts, as occur across the Moho discontinuity. This is an improvement over other similar methods (Vidale, 1988, 1990; Moser, 1991), which can encounter serious difficulties in the presence of sharp first-order contrasts. The model is discretized on an equally spaced grid comprised of constant velocity cells. Multiple arrivals (transmitted, diffracted, and head waves) are calculated at each grid node and the first arrival time is chosen. The time t at the current node is a function of the times t_n at some (3 or fewer) of the neighboring nodes and the slowness, s, in the cell traversed by the wavefront to reach this node. That is, $t=t\,(t_n, s)$. This method of travel time computation produces a full grid of travel times considerably faster than two-point ray tracing, and the sources and receivers can be located anywhere within the model. The

Podvin-Lecomte computations are output in the form of 3-D travel time tables, one for each station and seismic phase, which can be then used by a grid-search event location algorithm in lieu of global travel tables such as IASP91.

We have extended the P-L algorithm to compute the sensitivities of travel times to cell velocities, as required for the inversion. To calculate the ray path, we save the node pattern ("stencil") at each step through the model as we perform the normal P-L forward travel time calculation to predict arrival times. This stencil indicates which of the neighboring nodes were used to calculate the minimum time at the current node. The stencils can be used to reconstruct a path from any node of the grid to the source. The ray tracing is accomplished by identifying all of the grid nodes and the cells (slownesses) that contribute to the calculation of the time at the receiver. As the wave front propagates away from the source, more nodes (and cells) are involved in the travel time calculation at each step. After the midpoint of the ray path, the propagation region narrows until it reaches the one node at the source location. The sensitivity of the travel time to the slowness, $\partial t/\partial s$, is calculated at each grid node of the "ray" for the last cell traversed by the wavefront to reach that node. The weight of each neighboring node in the calculation of the time at the current node ($\partial t/\partial t_n$) determines the weight of the subsequent node-to-source subpath in the total travel time calculation for the ray. The sensitivities along each subpath are then weighted by this term.

Figure 2 shows XZ, YZ and XY projections of the ray sensitivity matrix at station ASH for an event on the Afghanistan-Pakistan border. Note that the ray paths are not straight lines but are instead "tubes" of the region that contribute to the calculation of the shortest travel time between two points. Figure 3 shows the sensitivities of the travel times calculated by P-L to cell slownesses for paths originating at station DSH in Tajikistan. The rays exhibit strong sensitivity to the model near the Moho boundary (presumably in the *Pn* velocity depth range). This suggests that updates to the *Pn* velocities as well as the Moho depth will provide the most significant improvement to the velocity model. After the sensitivities are calculated for all of the station Cartesian grids, they are then mapped to a geographic grid. Following this procedure *Pn* sensitivities are extracted to form the kernel matrix for the tomographic inversion.

The ray tracing algorithm and sensitivity calculation were tested for precision by comparing the travel time computed as the sum of the weighted sensitivity-slowness products to the forward P-L calculated times. For rays with 10^5 nodes, the difference between travel times calculated by these two methods is on the order of 10^{-2} s when the calculation is done in single precision. Error of this magnitude for the number of nodes in the ray can be accounted for by the level of precision in the calculation, demonstrating that the ray tracing technique is accurately tracing the minimum time P-L ray path.

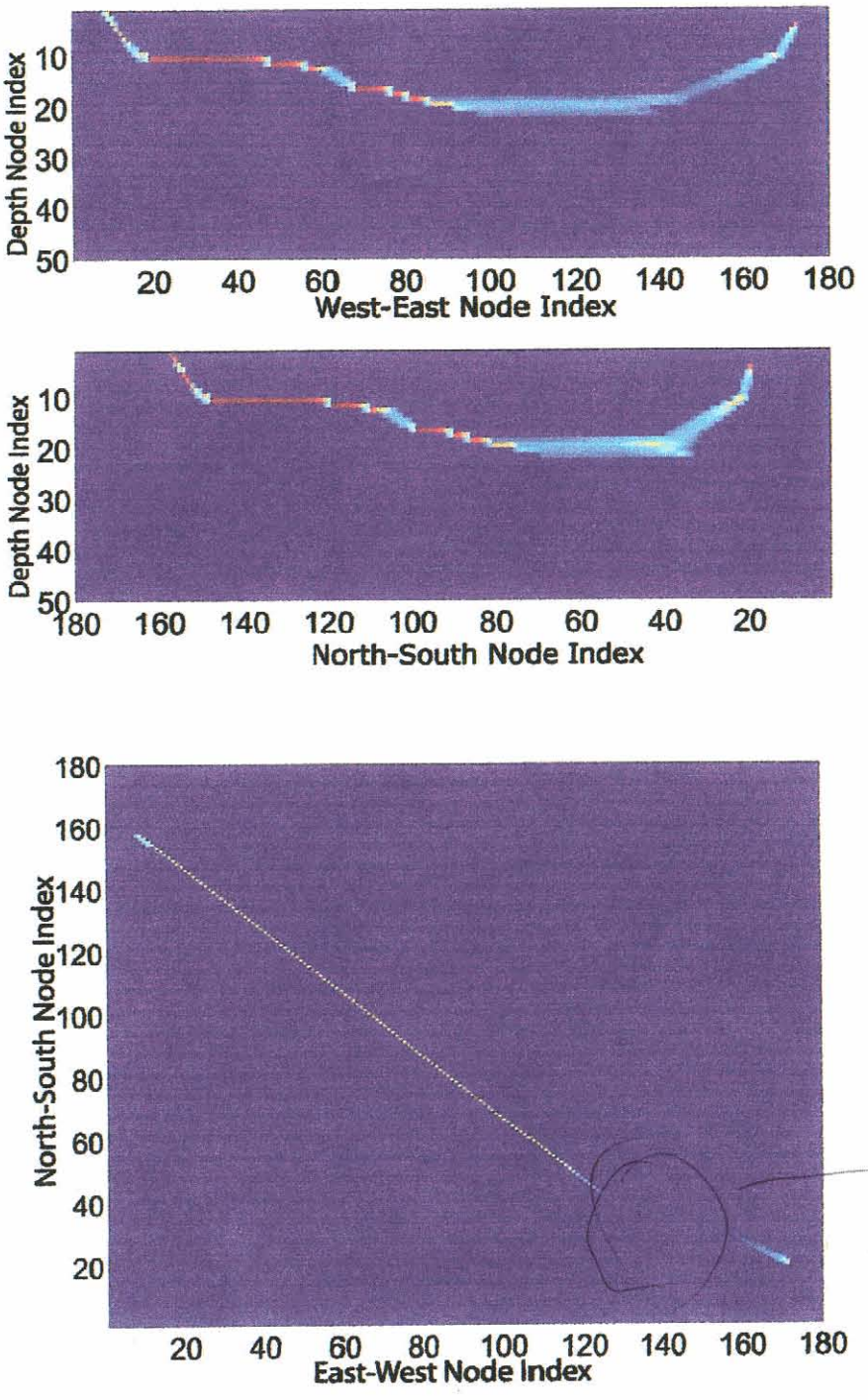

Figure 2: XZ (top), YZ (middle) and XY (bottom) projections of the ray path sensitivity matrix. This ray corresponds to an event near the Afghanistan/Pakistan border recorded at station ASH.

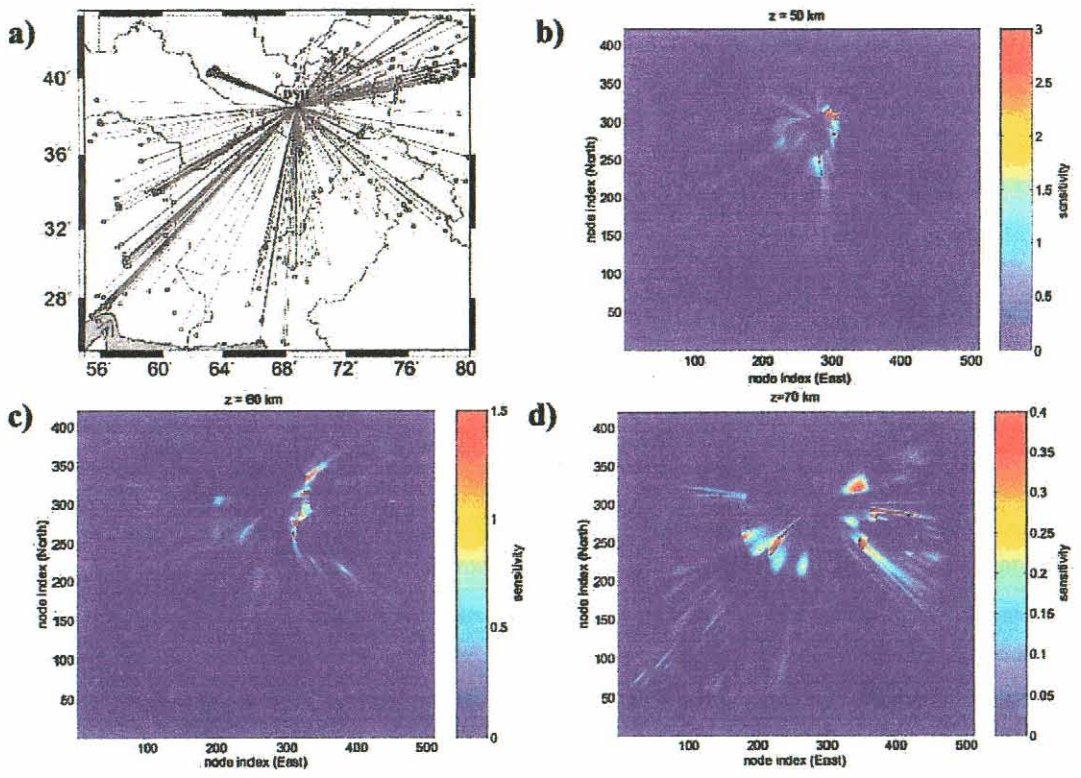

Figure 3: Ray path sensitivities calculated using the extended P-L algorithm. (a) Station DSH and events for which sensitivities were calculated shown with straight line approximations of the ray paths. (b), (c), and (d) Sensitivities from 50 km, 60 km and 70 km depth slices calculated for station DSH and events shown in panel (a). Note that the sensitivities are unitless. The sensitivities for all rays that encounter a cell are summed, producing scales that can range from zero upward. Deeper slices through the sensitivity matrix naturally have smaller scale ranges, since the rays spread out as they propagate away from the station.

3-D Grid Search Event Location

Our approach to seismic event location is based on a maximum-likelihood formulation. We define an optimal location for a seismic event to be that which maximizes a likelihood function, constructed on the basis of an assumed statistical model of errors in the seismic data. Confidence regions are defined in terms of hypothesis tests using likelihood ratios as the test statistics.

The origin parameters of a seismic event are a 3-D hypocenter vector **x** and an origin time *t*. Given *n* arrival time data, d_i, the location problem for the event may be expressed as

$$d_i = t + T_i(\mathbf{x}) + e_i, i = 1,\ldots,n \qquad (3)$$

where T_i is a travel time function (travel time table) for the ith datum, and e_i is the observational (picking) error. The index i counts over both stations and phase types (P, S, etc.).

Our grid search event location (GSEL) algorithm assumes the picking errors are statistically independent and have an *exponential power* distribution, whose probability density function (p.d.f.) is given by

$$f[e_i \mid \sigma_i] = \frac{1}{K(p)\sigma_i} \exp\left\{ -\frac{1}{p} \left| \frac{e_i}{\sigma_i} \right|^p \right\} \qquad (4)$$

where $p \geq 1$ and $K(p) = 2p^{1/p}\,\Gamma(1+1/p)$. A Gaussian p.d.f. results with p=2, and an exponential p.d.f. with p=1. We assume the standard errors, σ_i, are known within a constant factor and write

$$\sigma_i = \sigma \upsilon_i \qquad (5)$$

where the v_i are known but σ is not.

The unknowns in the single-event location problem are the origin parameters, $\mathbf{x}$ and t, and the standard error σ. We allow *a priori* constraints on σ, origin depth z and origin time t in the form of upper and lower bounds. The event epicenter can also be restricted to be within a specified distance of a given geographic location.

Considered as a function of the unknown parameters, the joint p.d.f. of the data defines a *likelihood* function, which we denote $L(\mathbf{x},t,\sigma \mid \mathbf{d})$. Our assumptions imply this function is given by

$$-\log L(\mathbf{x},t,\sigma \mid \mathbf{d}) = \sum_{i=1}^{n} \log \upsilon_i + n \log K(p) + n \log \sigma + \frac{1}{p\sigma^p} \Psi(\mathbf{x},t \mid \mathbf{d}) \qquad (6)$$

where Ψ is a *data misfit* function given by

$$\Psi(\mathbf{x},t \mid \mathbf{d}) = \sum_{i=1}^{n} \left| d_i - t - T_i(x) \right|^p \Big/ (\upsilon_i)^p \qquad (7)$$

The optimal estimates of the unknown parameters are those maximizing L, subject to the prior constraints. For $\mathbf{x}$ and t, this corresponds to minimizing Ψ and, in the Gaussian case p=2, to the method of nonlinear least squares. To determine the best-fitting $\mathbf{x}$ and t, GSEL employs a recursive grid-search technique.

Linear Conjugate Gradient Inversion

Once the database of events has been relocated using the appropriate travel time tables, and the ray path sensitivities have been transformed back onto a geographic grid, we perform a linear conjugate gradients inversion for an optimized update to the velocity model. We use a version of the LSQR algorithm (Nolet, 1983; Paige and Saunders, 1982) to produce this update. The LSQR algorithm is a linear conjugate gradient method used to iteratively solve large systems of sparse, linear equations. The output of the algorithm is a vector of changes to the input velocity model. The model update produced

by LSQR is constrained in several ways. First, we fix a small buffer region on the model region perimeter to the values of the initial model. This is to prevent large velocity variations from occurring in areas of the model that are not well covered by data and to allow us to seamlessly integrate our final models into other global models. Second, we apply a smoothing operator L (from Equation 2) to the model using a second differencing operator, which is equivalent to ensuring the curvature of the model is smooth (Twomey, 1977). Finally, we apply a scalar damping parameter to the model to balance the sharpness or noisiness with the horizontal spread or smoothness of the recovered velocity contrasts.

After the linear conjugate gradient method has converged to an optimized update to the model, we use the model change vector as a search direction in the next iteration of the NLCG inversion.

APPLICATION TO DATA FROM THE INDIA-PAKISTAN REGION

In this section we detail the application of our 3-D joint tomography and location algorithm to data from the India-Pakistan region. Figure 4 illustrates the setting of the WINPAK3D velocity model. The location of seismic station NIL at Nilore, Pakistan (future site of IMS station PRPK) is shown as the black triangle, and locations of the India and Pakistan nuclear test sites are shown as black stars. The area outlined with a black square is the contracted study region; the red rectangle outlines the region where we collected data to ensure sufficient data density for tomography inside the black square. Our study region, centered on Pakistan and extending into eastern Iran, the southern states of the Former Soviet Union, and western India, has a complex tectonic history that is exhibited in the diverse geometries of crustal structures across the area. Mountain ranges extend from the Kirthar Range in southern Pakistan across the Sulaiman Range of central Pakistan and continue eastward across the Salt Range in northern Pakistan and into the western Himalayas in India. These ranges represent a diffuse zone of deformation that is the result of the oblique continent-continent collision between India and Eurasia (Bernard *et al.*, 2000). Further complicating this deformation zone, a string of continental blocks, microcontinents, and island arcs have been incorporated along the Eurasian plate boundary (e.g., Powell, 1979; Klootwijk *et al.*, 1981; Cobbold and Davy, 1988; Haq and Davis, 1997). This deformation zone is bounded to the west by the Chaman fault, a large sinistral strike-slip fault.

The oceanic crust of the Arabian Sea plate contrasts the high mountain ranges and thick continental crust that characterize many areas within the India-Pakistan region. As a result, crustal thicknesses in this region vary widely from 15 km near the Arabian Sea (Byrne *et al.*, 1992) to more than 70 km under the Hindu Kush region (e.g., Brandon and Romanowicz, 1986; Fan *et al.*, 1994). In addition, there are several basin regions where thick sediments overlie much thinner continental crust than is typical of other parts of the region. The heterogeneous mix of crustal type, the variability of crustal thickness, and the

complex tectonic deformation make it difficult to accurately predict travel times in this region without a realistic regional velocity model.

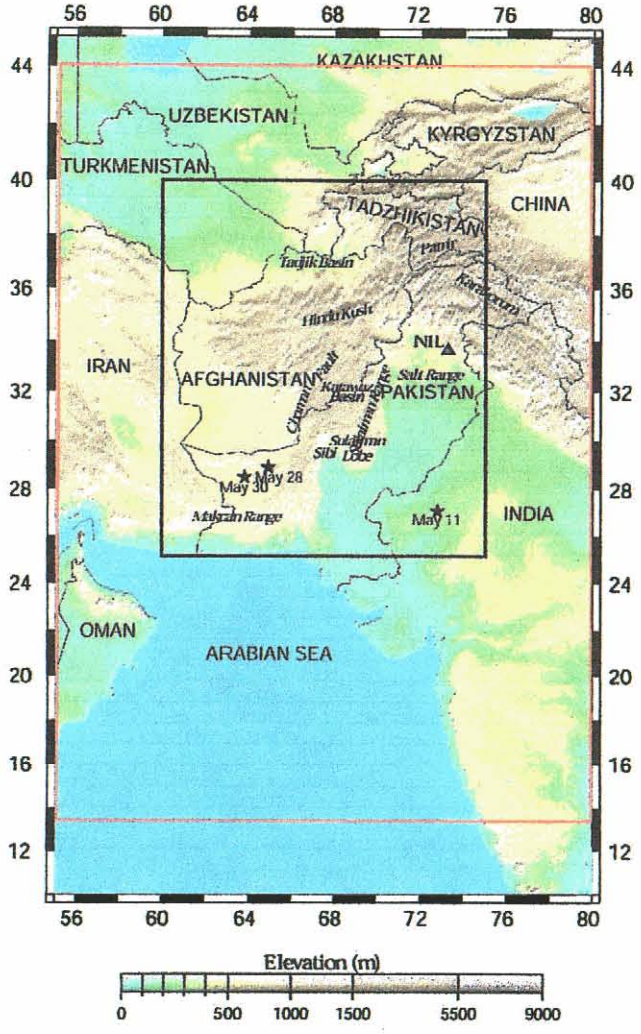

Figure 4: Physiographic map of the region of interest. The black rectangle outlines the area where the tomographically-derived velocity model is of the highest resolution; the red rectangle outlines the area where we collected data to ensure sufficient ray coverage in the tomography.

Initial Model

We compiled a detailed initial 3-D velocity model for the India-Pakistan region by synthesizing pertinent data from approximately sixty published references on the velocity structure, geology and tectonics throughout the region (Figure 4). The references we utilized included data such as seismic reflection and refraction surveys (i.e. DSS profiles, *Pn* tomography, *Pnl* waveform inversion), interpretations of gravity data, surface wave studies, and receiver function analyses. Because these data sources vary in spatial coverage, resolution, and the number of constraints, the model varies in a similar manner. The velocity model is defined on a grid of one-degree by one-degree blocks and 5 km

depth intervals from 0 to 75 km. We appended the IASP91 model (Kennett and Engdahl, 1991) to the base of the preliminary velocity model, beginning at 80 km depth and extending to 700 km depth, to accommodate ray paths that travel into the upper mantle. Figure 5 shows depth slices of our initial velocity model at 0, 20, 40 and 60 kms

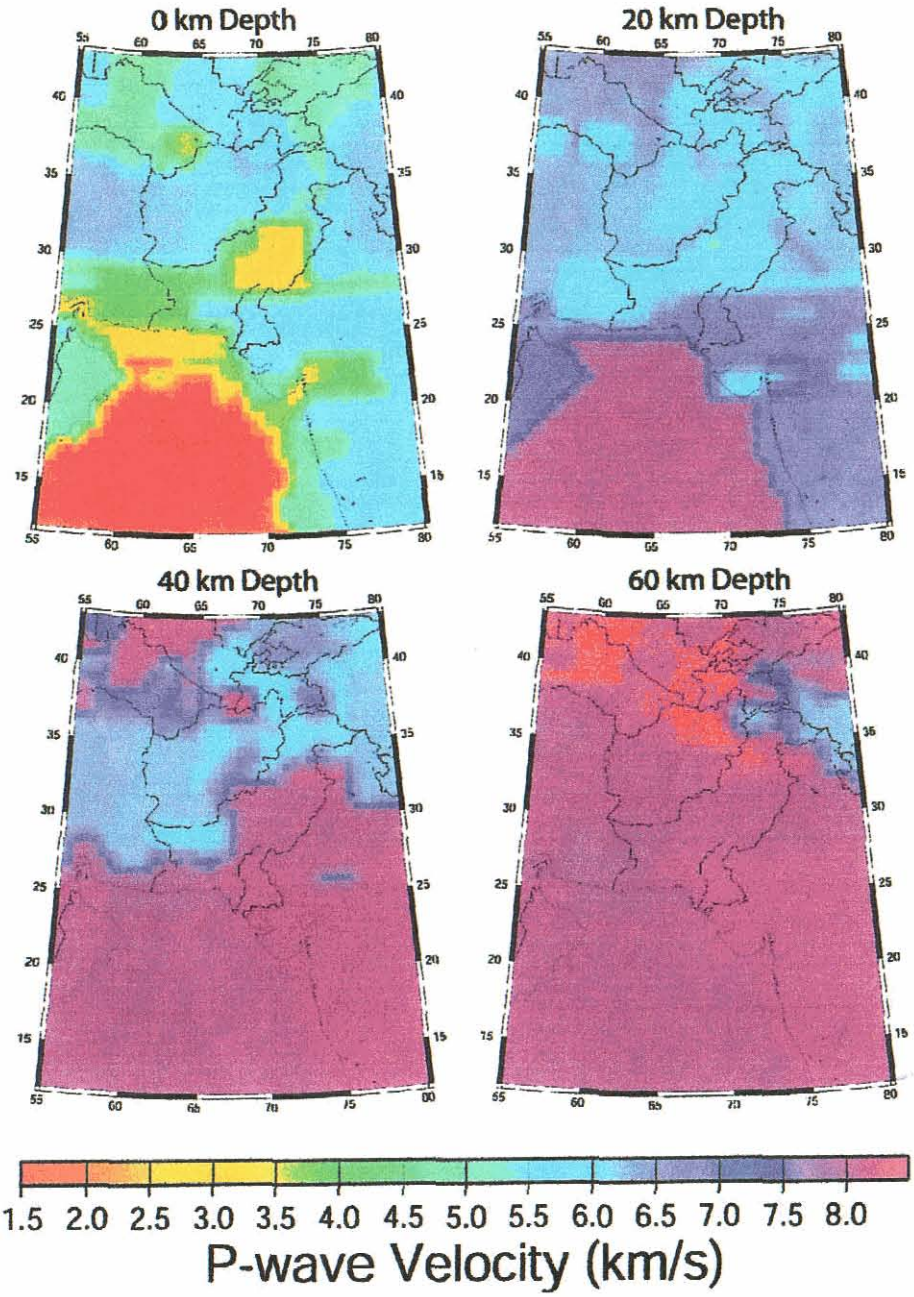

Figure 5: Depth slices at 0 km, 20 km, 40 km, and 60 km through the initial model for the India-Pakistan model. There is considerable variability in the crust and upper mantle region.

depth showing the variability of velocity model resolution, as well as the range of crustal thickness across our study region. Some preliminary validation was performed on the initial model to verify its suitability and potential to improve event locations. See Johnson and Vincent (2001) for details on the development and validation of this initial WINPAK3D model.

Earthquake Dataset

Our data set is made up of events selected from the Engdahl *et al.* (1998) database (EHB) of well-located earthquakes and explosions. The EHB data set is considered to be GT15 or better in continental areas, according to the IASPEI Working Group on Reference Events (http://lemond.colorado.edu/~copgte/). We chose our particular subset of events from the EHB database based on their spatial distribution across the region, both in latitude/longitude and depth. Only events with 6 or more regional arrivals were selected from the database to insure sufficient data during the hypocenter location phase of the inversion. In addition, we selected only those arrivals with residuals smaller than 7 seconds (i.e. greater than -7 and less than +7 seconds), in an effort to filter out data with potentially bad arrival time picks or incorrect phase assignments. The value of 7 seconds was chosen to optimize maximum retention of data, while still removing the bulk of the poor arrival readings. We did not lower the residual cut-off too much because residuals of 5 seconds or greater are possible in parts of the model such as the Hindu Kush region. Figure 6 shows the histogram of the residuals in our data set; these consist of the observed arrival times minus IASP91 predicted arrival times. By choosing a cut-off of 7 seconds, we retain 96.5% of the data while removing those data with abnormally high residuals. The events in the data set were recorded at 70 stations within our model region, and consisted of 6,626 arrivals that were used in the joint inversion. Figure 7 depicts the ray coverage of our data set, color coded by epicentral distance (Δ). We show the data set divided into bins of 5° to demonstrate that the rays to be used in the tomographic inversion are of the appropriate epicentral distance to adequately sample the *Pn* velocity.

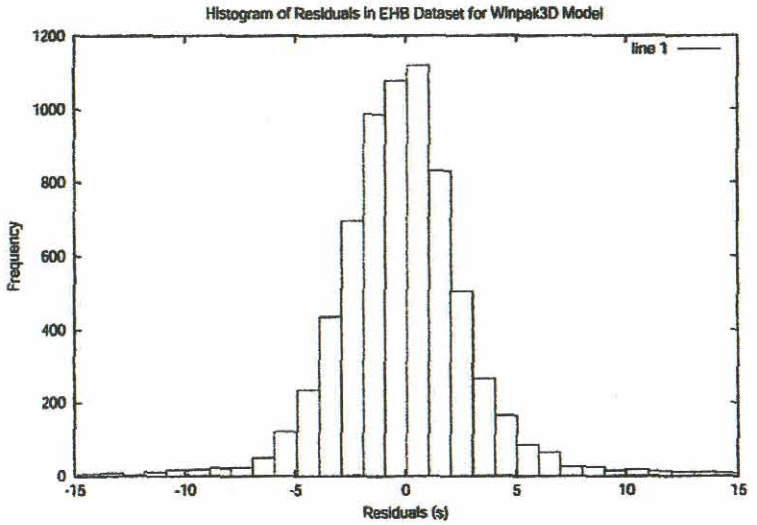

Figure 6: Histogram of residuals in the tomography data set. We retained data that had residuals of 7 seconds or less to reduce the number of incorrect arrival readings.

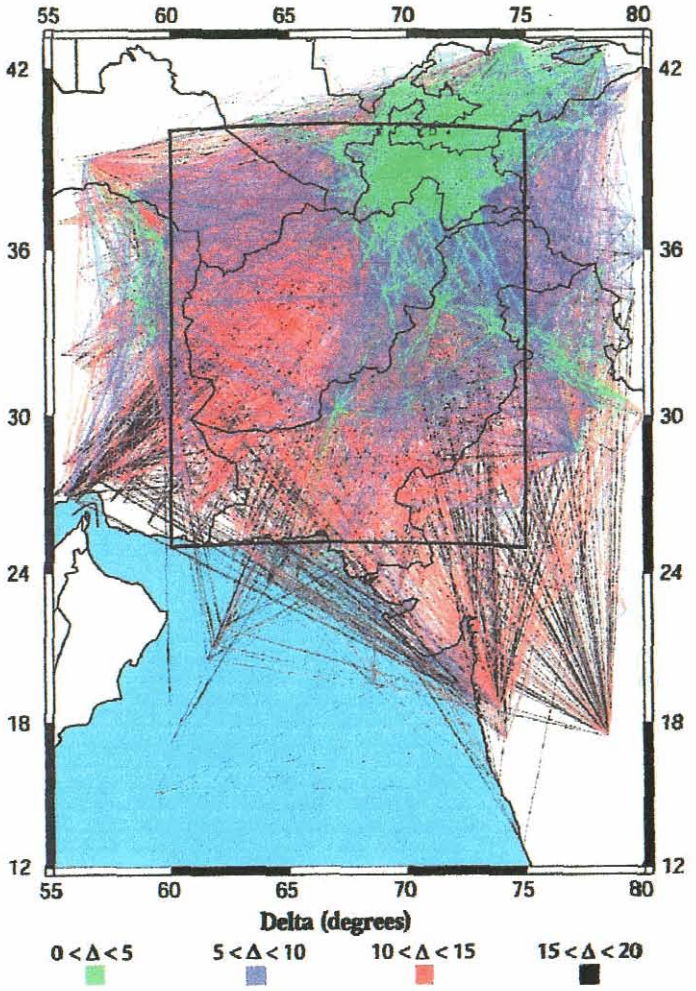

Figure 7: Ray coverage (straight line approximations) of the earthquake data set used to produce a tomographic update to the Pn *velocity over the model region. The ray colors correspond to the distance between station and event, and demonstrate the usefulness of the data set to sample* Pn *adequately.*

Resolution Test

Prior to inverting for the India-Pakistan *Pn* velocity map, we conducted a resolution test of the data set to estimate the ability of the algorithm to recover a checkerboard pattern using our station/event geometry. We overlaid a checkerboard model (shown on the left in Figure 8) across the region and produced 3-D synthetic travel times for all the station-event pairs in our earthquake data set. Each square in the checkerboard model has a size

of 3° in latitude and 3° in longitude. Alternating checkers have constant velocities of 7.9 km/s and 8.3 km/s, with a transition border set to the midpoint between high and low velocities between all checkers. Using the synthetic travel times and a constant velocity initial model (the IASP91 *Pn* velocity of 8.04 km/s), we performed one iteration of our nonlinear conjugate gradient scheme to retrieve an estimate of the resolving capability of our data set. The damping parameter was chosen to reduce the rms while keeping the noise (one-node variations) low. The damping parameter chosen also preserves the amplitude of the velocity variations of the synthetic model. The pattern recovered from the inversion is on the right in Figure 8, with our specific region of interest outlined in black (between 25-40°N, 60-75°E). Resolution is excellent in the outlined region, while less well-resolved regions to the south and northwest reflect the reduced data coverage.

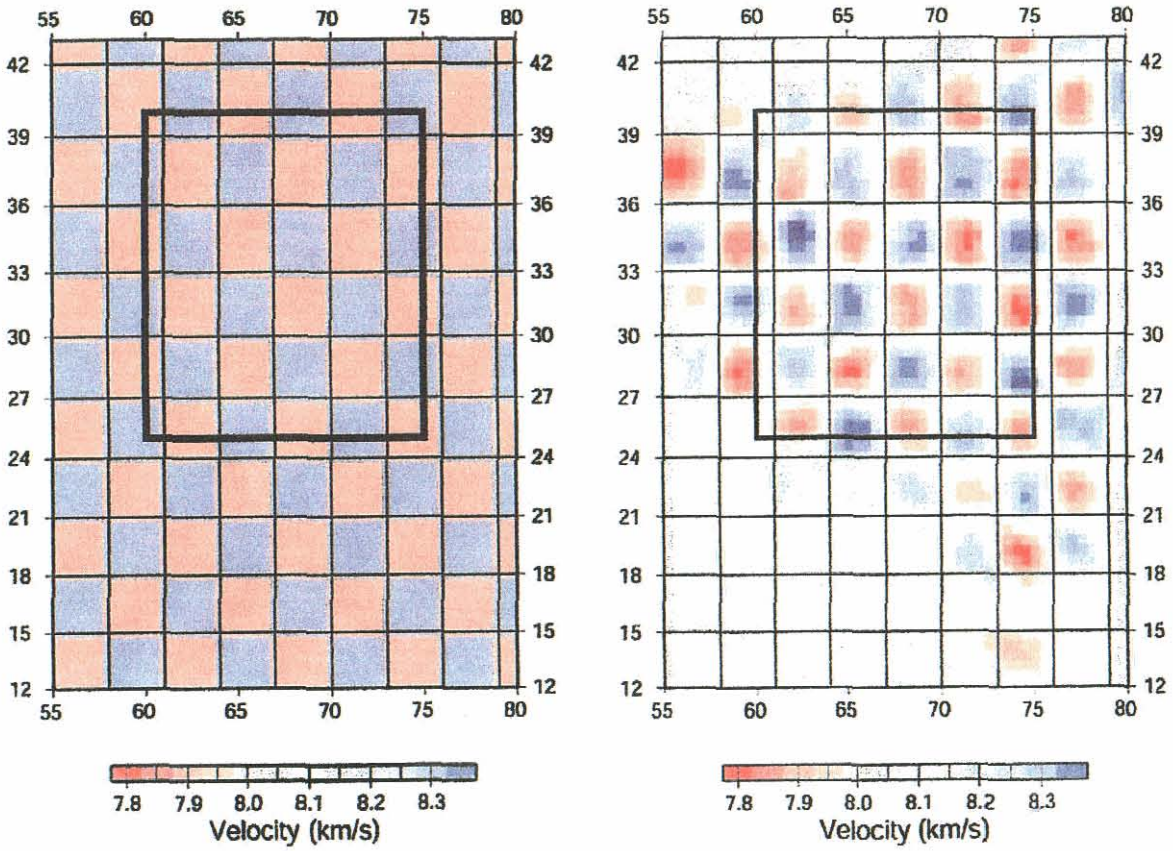

Figure 8: Results from performing a checkboard resolution test of our earthquake data set. On the left is the model we used to predict synthetic travel times from events to stations in our data set. On the right is the checkerboard pattern resolved by one iteration of the nonlinear inversion method. Inside the region of interest (outlined in black), the resolution of the individual checkers is excellent.

Pn Inversion Results

After the checkerboard resolution test, we performed several iterations of our nonlinear inversion technique to invert for an update to the *Pn* velocity map extracted from our initial model. The event hypocenters were constrained to be within15 km of the EHB locations, to correspond with their GT15 designation. The damping parameter for the inversions was again chosen to reduce the rms while keeping the noisiness of the recovered velocity change low. Figure 9 shows the initial *Pn* map on the left and the model retrieved by the inversion procedure on the right. The general distribution of lower and higher velocities in the final model is similar to the starting model, but contains more detail. The RMS fit to the data of the final model is 1.81, which is a significant. improvement over both the IASP91 value of 2.42 and the starting model value of 2.01. Table 1 lists the RMS values from the IASP91 model (for comparison) and each iteration of the nonlinear algorithm.

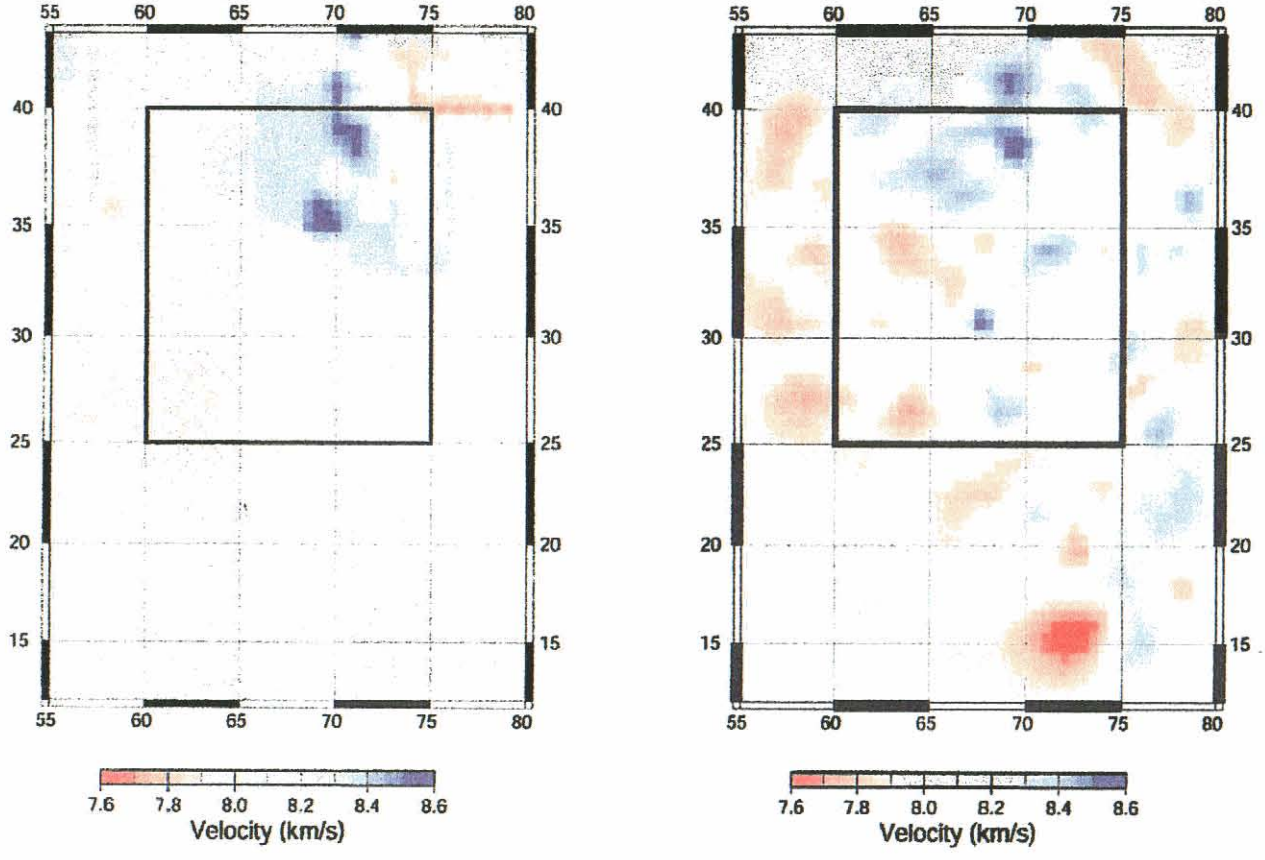

Figure 9: Initial (left) and final (right) Pn *velocity maps. The final Pn velocity model was the result of three iterations of our nonlinear tomography scheme.*

Iteration #	RMS	Reduction in RMS
IASP91	2.42	N/A
W0	2.01	0.41
W1	1.92	0.09
W2	1.85	0.07
W3	1.82	0.03

Table 1: The RMS results from several iterations of the joint nonlinear inversion method. The first row entry is provided for comparison with the 1-D IASP91 global model.

In the region contained within the black rectangle, we feel that the data coverage is excellent and the *Pn* velocity changes are reliable. However, one area of the model that cannot be considered reliable is to the southeast on the continent of India. This region seems well resolved on the checkerboard model (Figure 8), but is overestimated in the updated velocity map (Priestley *et al.*, 2001). High velocities in this region can be explained by both poor data coverage (see the ray coverage picture) and by the fact that our real data have errors, while synthetic data do not. We are currently acquiring additional seismic data in the region and plan to reevaluate the results in the future.

It is somewhat surprising that the final model was reached in only three iterations of the nonlinear technique, given the scale and underdetermined nature of the tomography problem. One possible explanation for this is the high quality of the initial model, which has been shown to improve seismic event locations in the region. Also, it is probable that inverting strictly for the *Pn* velocity without allowing for changes in the crustal velocities and Moho interface depth is hampering further decreases in the residuals. Finally, it is also possible that unknown picking errors exist in the data that preclude further improvement in the velocity model. Without having the waveform data available to repick the phases, we cannot estimate the effect these errors have on the inversion process or final model.

After the third iteration of the nonlinear inversion method, we reinserted the final update for the *Pn* velocity map into our 3-D velocity model for the Pakistan region. We then performed some preliminary validation on the model to verify that it improves regional seismic event location.

Preliminary Model Validation

There is very little ground truth data currently available in our region that can be used to validate our 3-D model. However, on 14 February 1977, a magnitude 5.2 earthquake occurred in the region near Nilore, Pakistan that was well recorded by the Tarbela and Chasma local networks. Based on data from these networks, Seeber and Armbruster (SA) (1979) found a hypocenter for the event and conducted a detailed study of the aftershock sequence. Using teleseismic as well as regional data, both the ISC and the

USGS (NEIC) located the event within about 5 km of the epicenter reported by SA, who used only the local network data. The ISC calculated the depth of the event to be 27 km, and the USGS fixed the depth at 33 km. However, the hypocenters of the main shock (14.5 km) and the 50 accurately located aftershocks determined by SA indicate a rupture surface between 12 and 18 km depth.

Because of the regional station coverage and the further constraint on the hypocentral region derived from the aftershock study, the 14 February 1977 event (denoted the VDAY event) has one of the best constrained locations in the region. Therefore, we began preliminary testing of the location capability of our updated velocity model using a subset of regional stations from this event. Figure 10 shows the regional stations that were used to locate the VDAY event; the maximum azimuthal gap is 140°. We used 3-D travel time tables from both our final WINPAK3D model and the 1-D IASP91 model in GSEL to locate the VDAY event.

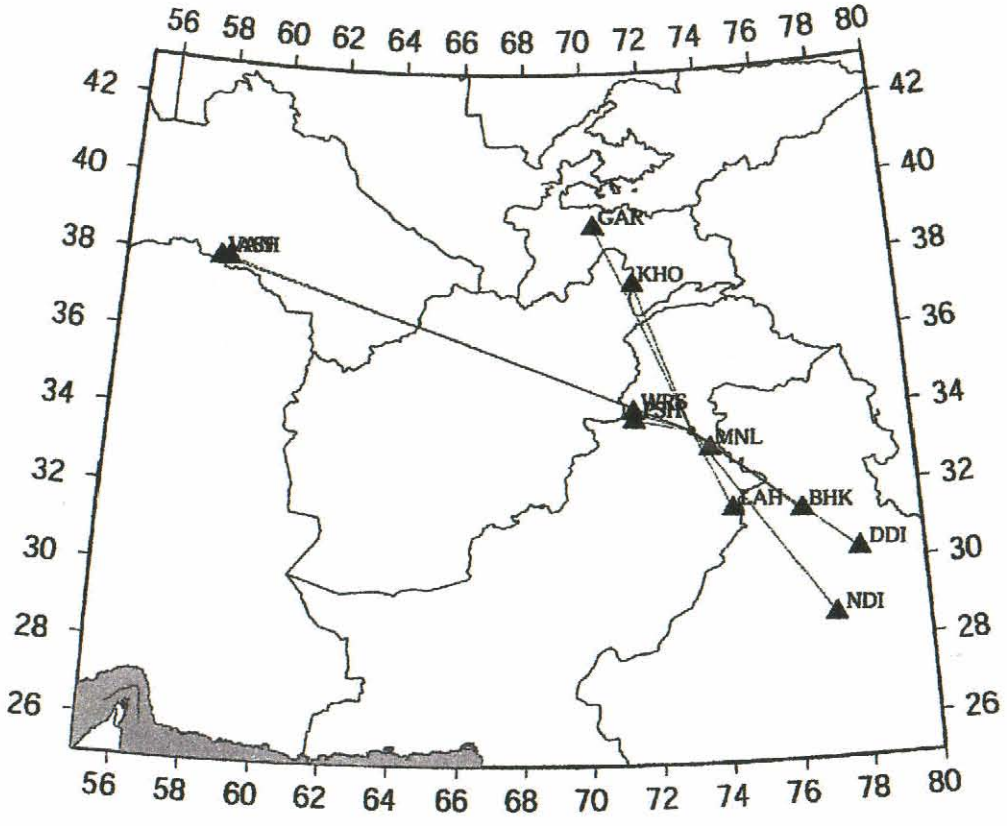

Figure 10: Eleven regional stations used to locate the VDAY event using both the IASP91 model and the initial and final WINPAK3D models.

Figure 11 shows the hypocenters from the VDAY event, calculated using data from these 11 regional stations, for the updated WINPAK3D model (blue x), initial WINPAK3D model (red x), and the 1-D IASP91 model (green x). We compare these solutions with the SA location for this event (black star). The surface and depth projections of the respective three-dimensional confidence regions determined by Monte Carlo simulation (Rodi and Toksöz, 2000) show the 95% confidence levels for each model's hypocenter. The epicenter mislocation of the updated WINPAK3D model from the SA event location is 3.5 km, while the initial model's epicenter mislocation is 9.3 km and the IASP91 epicenter mislocation is 31.7 km. In addition, the 95% confidence region for both the initial and updated WINPAK3D model epicenters encompass the SA epicenter while the 95% confidence region for the IASP91 epicenter does not.

Also shown in Figure11 are the hypocenters determined by both the ISC and the USGS (NEIC) (open circles) using teleseismic data as well as regional data. Note that by using regional data alone, the 3-D model is able to estimate the hypocenter of this event as well as the teleseismically-derived estimates. These results are encouraging for the potential success of using 3-D regional velocity models to find accurate locations of small events that are not recorded teleseismically.

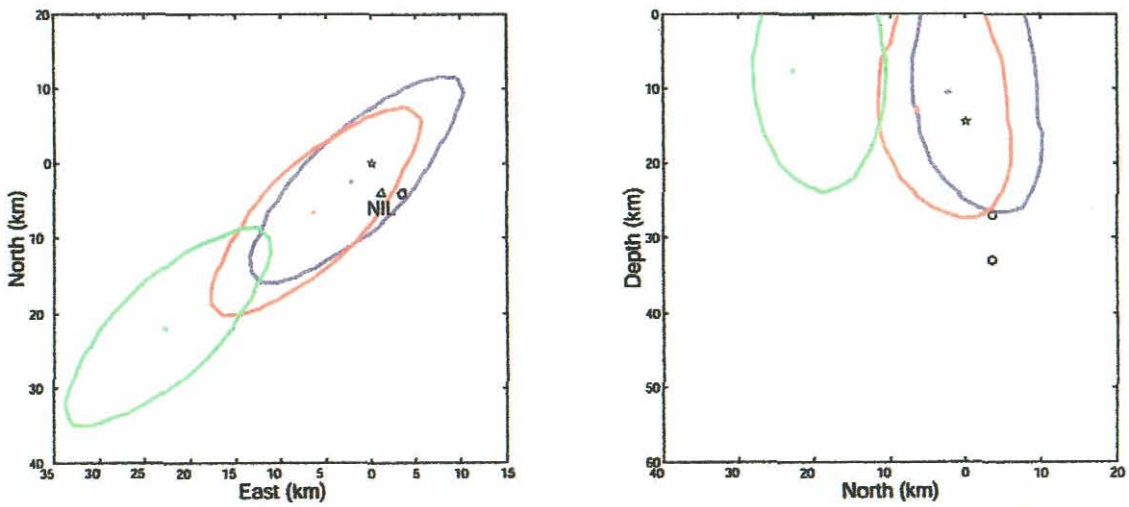

Figure 11: Hypocenters from the VDAY event, calculated using data from 11 regional stations, for the updated WINPAK3D model (blue x), initial WINPAK3D model (red x), and the 1-D IASP91 model (green x). We compare these solutions with the SA location for this event (black star). Also shown are the hypocenters determined by both the ISC and the USGS (NEIC) (open circles) using teleseismic data as well as regional data.

Figure 12 shows a source-specific station correction (SSSC) derived from the WINPAK3D regional velocity model for the India-Pakistan region for a source at 15 km depth. This correction surface was produced by calculating travel times from the surface at the Nilore (NIL) station to all other points in the 3-D model, which was discretized on a 5 km grid. We then subtracted the travel times through the IASP91 model, which we

discretized onto an equivalent 5 km grid and derived using the identical PL travel time prediction method. Figure 12 represents the anticipated station correction with respect to the IASP91 model for an event occurring at 15 km depth beneath station NIL.

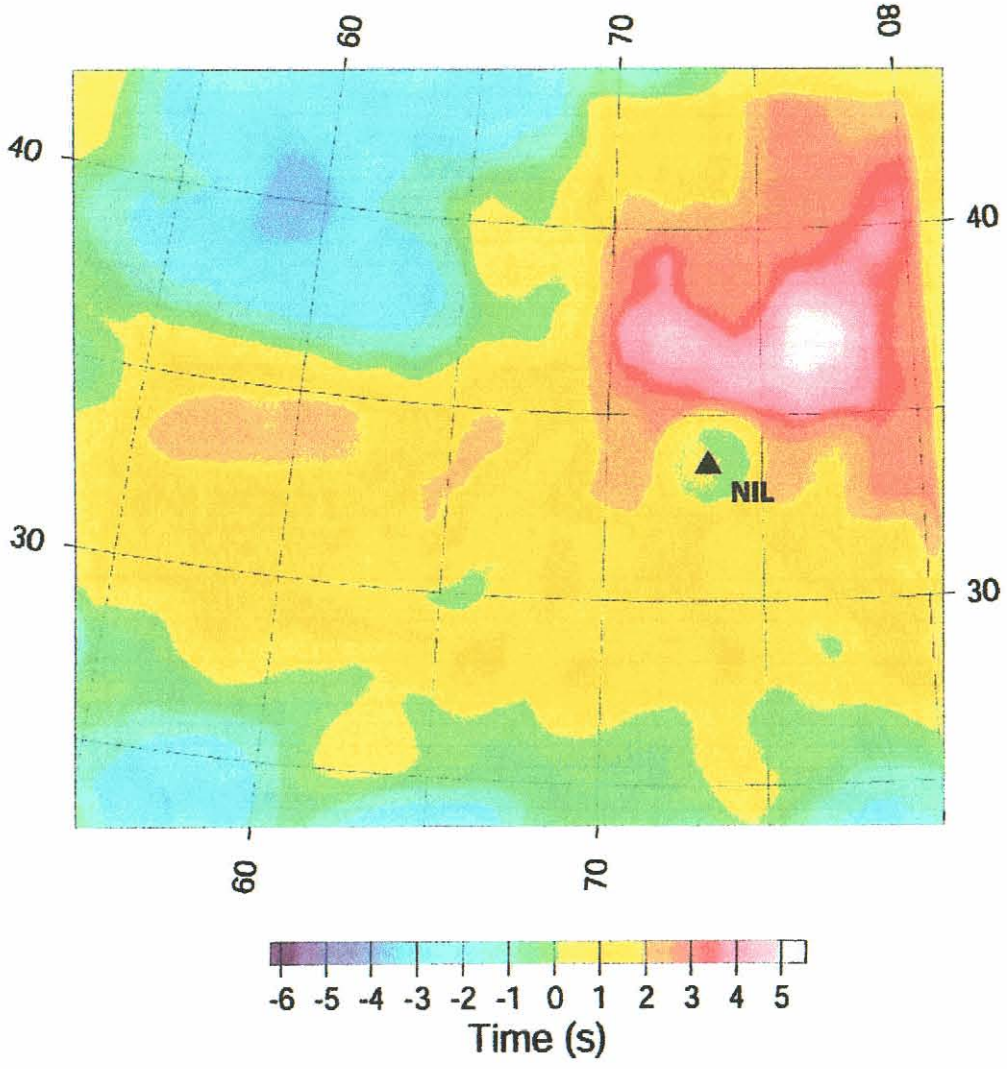

Figure 12: Model-based source specific station correction (SSSC) at station NIL for events occurring at 15 km depth.

Since the VDAY event occurred near the Nilore station, it provides a unique reciprocity test of our 3-D velocity model. Stations that recorded the event in other parts of our model act as sources that could potentially propagate seismic energy to the station at Nilore. We analyzed the residuals from this event and compared them with the SSSC derived from the WINPAK3D model. In Figure 13 we show this comparison, which illustrates the difference between the empirical travel time corrections (residuals) and the corrections derived from the WINPAK3D model. The two are in overall agreement, with absolute differences generally from 0 to 3 seconds. Note that SSSCs can range up to 8 seconds in some regions. For approximately half the stations, we have a less than 1 second difference.

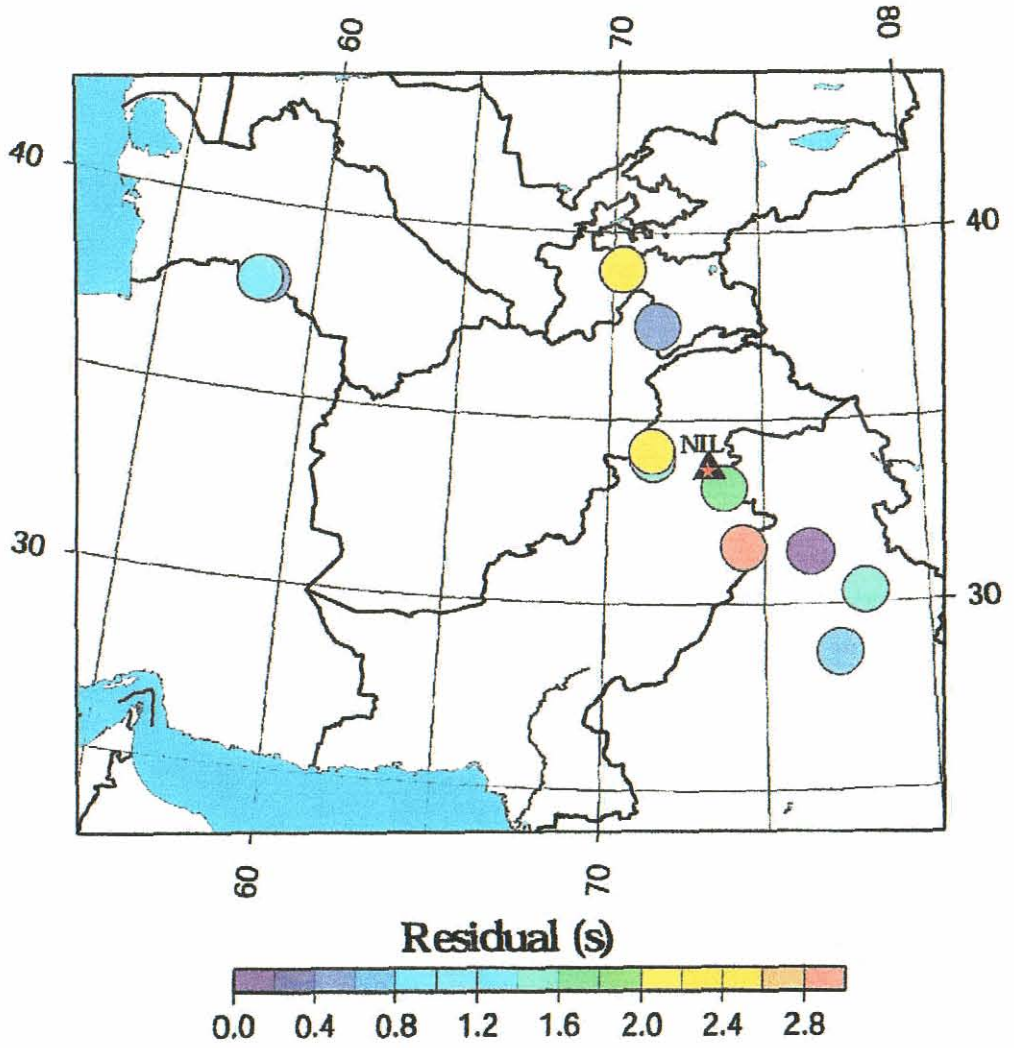

Figure 13: Differences between empirical travel time corrections (residuals) and the corrections derived from the WINPAK3D model for all 23 regional stations used to locate the VDAY event.

CONCLUSIONS AND RECOMMENDATIONS

Our primary goal in this project was to develop a 3-D model of the crust and upper mantle in the Pakistan region to improve regional seismic event location. We developed our 3-D model by applying a joint velocity tomography and event location procedure to a dataset of earthquakes from the region. The model was iteratively updated using a nonlinear, conjugate-gradients technique that adjusts the velocity model to minimize the misfit between calculated and observed travel times from multiple stations and events, subject to smoothness constraints. We performed several iterations of this nonlinear algorithm to invert for the *Pn* velocity as a function of latitude and longitude and then

imposed a fixed rule for extrapolating this velocity into the upper mantle. Our results show that the new model fits the data better compared to both the initial model and the global 1-D IASP91 model. The root mean square (RMS) error for the updated 3-D model is 1.81, compared to 2.01 for the initial 3-D model and 2.42 for the IASP91 model. Preliminary validation of the model indicates that it does improve regional seismic event location.

This algorithm can be effectively transported for use in other regions of the world and has already been applied to the area surrounding the IMS station BRVK at Borovoye, Russia (Murphy *et al.*, 2001). It is currently one of the most powerful methods available to produce tomographic 3-D regional velocity models. These models can then be used to generate source-specific station corrections (SSSC's) for use in accurate regional and teleseismic event locations. We plan further extensions to the method, including allowing for more flexible changes in the upper crust and mantle portions of the model and improving the ray tracing algorithm.

REFERENCES

Bernard M., B. Shen-Tu, W.E. Holt, and D.M. Davis (2000). Kinematics of active deformation in the Sulaiman Lobe and Range, Pakistan, *J. Geophys. Res.*, **105**, 13,253-13,279.

Brandon, C. and B. Romanowicz (1986). A "no-lid" zone in the Central Chang-Thang platform of Tibet: Evidence from pure path phase velocity measurements of long period Rayleigh waves, *J. Geophys. Res.*, **91**, 6547-6564

Byrne, D.E., L.R. Sykes, and D.M. Davis (1992). Great thrust earthquakes and aseiemic slip along the plate boundary of the Makran subduction zone, *J. Geophys. Res.*, **97**, 449-478.

Cobbold, P.R. and P. Davy (1988). Indentation tectonics in nature and experiment, 2, Central Asia, *Bull. Geol. Inst. Univ. Uppsala, New Series,* **14**, 143-162.

Dewey, J. W. (1972). Seismicity and tectonics of western Venezuela, *Bull. Seism. Soc. Am.* **62**, 1711-1751.

Douglas, A. (1967). Joint epicentre determination, *Nature* **215**, 47-48.

Engdahl, E. R. and W. H. K. Lee (1976). Relocation of local earthquakes by seismic ray tracing, *J. Geophys. Res.* **81**, 4400-4406.

Engdahl E. R., R. van der Hilst, and R. Buland (1998). Global teleseismic earthquake relocation with improved travel times and procedures for depth determination, *Bull. Seism. Soc. Amer.* **88** (3), 722-743.

Fan, G., J.F. Ni, and T.C. Wallace (1994). Active tectonics of the Pamirs and Karakorum, *J. Geophys. Res.*, **98**, 12,057-12,082.

Haq, S.S.B. and D.M. Davis (1997). Oblique convergence and the lobate Mountain belts of western Pakistan, *Geology*, **25**, 23-26.

International Association of Seismology and Physics of the Earth's Interior (6/27/00), Working Group on Reference Events (available from http://lemond.colorado.edu/~copgte/).

Johnson, M. And C. Vincent (2002). A Case Study in the Development and Validation of a 3-D Initial Model for Tomographic Studies, *Bull. Seism. Soc. Amer.* In Review.

Jordan, T. H. and K. A. Sverdrup (1981). Teleseismic location techniques and their application to earthquake clusters in the south-central Pacific, *Bull. Seism. Soc. Am.* **71**, 1105-1130.

Kennett, B.L.N. and E. R. Engdahl (1991). Travel times for global earthquake location and phase identification, *Geophys. J. Int.* **105**, 429-465.

Klootwijk, C.T., R. Nazirullah, K.A. DeJong, and H. Ahmed (1981). A paleomagnetic reconnaissance of northeastern Baluchistan, Pakistan, *J. Geophys. Res.*, **86**, 289-306.

Lomax, A. (1999), Probabilistic, non-linear earthquake location in 3-D media (An online guide to software), http://iapetus.unice.fr/~lomax/nlloc.

Moser, T.J. (1991), Shortest path calculation of seismic rays, *Geophysics*, **56**, pp. 59-67.

Murphy, J., W. Rodi, M. Johnson, I. Kitov, J. Sultanov, B. Barker, C. Vincent, V. Ovtchinnikov, and Y. Shchukin (2001). Seismic Calibration of Group One International Monitoring System Stations in Eastern Asia for Improved Event Location, *Proceedings*, 23rd Annual DoD/DOE Seismic Research Review.

Nolet, G (1983). Inversion and resolution of linear tomographic systems (abstract). *Eos, Trans. Am. Geophys. Union*, **74**, 775-6.

Paige, C.C., and M.A. Saunders (1982). LSQR: An algorithm for sparse linear equations and sparse least squares, *ACM Transactions on Mathematical Software*, March 1982.

Pavlis, G. L. (1992). Appraising relative earthquake location errors, *Bull. Seism. Soc. Am.* **82**, No. 2, 836-859.

Podvin, P. and I. Lecomte (1991). Finite difference computation of travel times in very contrasted velocity models: a massively parallel approach and its associated tools, *Geophys. J. Int.* **105**, 271-284.

Powell, C. (1979). A speculative tectonic history of Pakistan and surroundings: Some constraints from the Indian Ocean, in *Geodynamics of Pakistan*, edited by A. Farah and K. DeJong, 5-24, Geol. Surv. Of Pakistan, Quetta.

Priestley, K., V. Gaur, S. Rai, J. Bonner and J. Lewkowicz (2001). Broadband Seismic Studies in Southern Asia, *Proceedings*, 23rd Annual DoD/DOE Seismic Research Review.

Reiter, D., C. Vincent, M. Johnson, J. Bonner, and W. Rodi (2001). Methods of Improving Regional Seismic Event Locations, *Proceedings*, 23rd Annual DoD/DOE Seismic Research Review.

Rodi, W. and M.N. Toksöz (2000). Grid-search techniques for seismic event location, *Proceedings*, 22nd Annual DoD/DOE Seismic Research Symposium.

Rodi, W.L., J.F. Masso, J.M. Savino, T.H. Jordan and J.B. Minster (1981), Relocation of earthquakes in eastern Washington based on a three-dimensional velocity model, *Final Technical Report* SSS-R-81-4857, S-Cubed, San Diego.

Seeber, L. and J. Armbruster (1979). Seismicity of the Hazara Arc in northern Pakistan: decollement vs basement faulting, in *Geodynamics of Pakistan*, A. Farah and K. A. DeJong (Editors), *Geological Survey of Pakistan*, 131-142.

Spencer, C. and D. Gubbins (1980), Travel-time inversion for simultaneous earthquake location and velocity structure determination in laterally varying media, *Geophys. J. R. Astr. Soc., 63*, pp. 95-116.

Twomey, S. (1977). Introduction to the Mathematics of Inversion in Remote Sensing and Indirect Measurements. Elsevier, Amsterdam.

Vidale, J. (1988), Finite difference calculations of travel times *Bull. Seismol. Soc. Amer.*, **78**, pp. 521-526.

Vidale, J. (1990), Finite-difference calculation of traveltimes in three dimensions, *Geophys.*, **55**, pp. 521-526.

DEPARTMENT OF DEFENSE

DEFENSE TECHNICAL INFORMATION CENTER
8725 JOHN J. KINGMAN ROAD,
SUITE 0944
FT. BELVOIR, VA 22060-0944
2 CYS ATTN: DTIC/OCA

DEFENSE THREAT REDUCTION AGENCY
8725 JOHN J. KINGMAN ROAD MS 6201
FT. BELVOIR, VA 22060-6218
2 CYS ATTN: TDND/ D. BARBER

DEPARTMENT OF DEFENSE CONTRACTORS

ITT INDUSTRIES
ITT SYSTEMS CORPORATION
1680 TEXAS STREET, SE
KIRTLAND AFB, NM 87117-5669
2 CYS ATTN: DTRIAC
ATTN: DARE

WESTON GEOPHYSICAL CORPORATION
57 BEDFORD STREET
SUITE 102
LEXINGTON, MA 02420
ATTN: D. REITER

MASSACHUSETTS INSTITUTE OF TECHNOLOGY
EARTH RESOURCES LABORATORY
42 CARLETON STREET
CAMBRIDGE, MA 02142
ATTN: W. RODI